Single Molecule Detection of Nanomechanical Motion

Vadim Puller,[1,2] Brahim Lounis,[3] and Fabio Pistolesi[1,2]
[1]Université Bordeaux, LOMA, UMR 5798, F-33400 Talence, France
[2]CNRS, LOMA, UMR 5798, F-33400 Talence, France
[3]LP2N, Université Bordeaux, Institut d'Optique & CNRS, UMR 5298, F-33405 Talence, France
(Received 27 November 2012; published 19 March 2013)

We investigate theoretically how single molecule spectroscopy techniques can be used to perform fast and high resolution displacement detection and manipulation of nanomechanical oscillators, such as singly clamped carbon nanotubes. We analyze the possibility of real time displacement detection by the luminescence signal and of displacement fluctuations by the degree of second order coherence. Estimates of the electromechanical coupling constant indicate that intriguing regimes of strong backaction between the two-level system of a molecule and the oscillator can be realized.

DOI: 10.1103/PhysRevLett.110.125501 PACS numbers: 81.07.Oj, 07.10.Cm, 37.10.De, 42.50.Hz

Introduction.—Perfecting displacement detectors is the central motivation driving the research in nanomechanics [1] and a necessary step toward quantum manipulation of mechanical degrees of freedom. The main strategy is to couple the mechanical oscillator to a well controlled quantum system whose state can then be very accurately measured. A nonexhaustive list of such detection systems includes single-electron transistors [2], SQUIDs [3], qubits [4], point contacts [5], optical cavities [6], and microwave cavities [7]. A wide range of possibilities is opened by the emergence of a new class of detectors, where the displacement of the nano-oscillator modulates the energy splitting of a two-level system (TLS) [8,9], which is then measured via optical resonance spectroscopy. In Ref. [8], the displacement (x) of the nano-oscillator is detected by exploiting a Zeeman split TLS (nitrogen vacancy center) embedded in the tip of the oscillator moving in a strongly inhomogeneous magnetic field.

In this Letter we propose using the single molecule spectroscopy [10–12] to detect the displacement of nano-oscillators, such as carbon nanotubes suspended from the tip of an atomic force microscope (AFM), see Fig. 1. At liquid helium temperatures, the zero-phonon lines of single molecule fluorescence excitation spectra are extremely narrow, since the dephasing of optical transition dipole due to phonons vanishes. For well chosen fluorophores or matrix systems [10], such as the dibenzo-anthanthrene embedded in a n-hexadecane Shpol'skii matrix, the zero phonon line has a spectral width limited by the lifetime of the molecule excited state ($\sim$ 10–20 MHz) [11,12]. Under an external electric field, centrosymmetric molecules such as dibenzo-anthanthrene usually gain permanent dipole moments due to distortions induced by the surrounding solid matrix. This leads to a linear contribution to the Stark shift, which is usually much stronger than the quadratic contribution. In disordered matrices, such as in polymers, the permanent electric dipole moment can be as large as 1D and is around 0.3D in a n-hexadecane Shpol'skii matrix [corresponding to $\sim$3 MHz/(kV/m)] [12]. This allows one to use single molecules as highly sensitive probes of their nanoenvironment and of local electric fields [13,14].

By setting a bias voltage between the nanotube (NT) and the conducting (and transparent) substrate, it is possible to generate an electric field between the NT tip and the substrate at the limit of the discharge field $E_c = 10^7$ V/m [15], with a very large radial gradient of the order of $E_c/R = 10^{16}$ V/m^2, where $R \approx 1$ nm is the NT radius [16]. Any small displacement of the NT will thus induce a large modulation of the molecular Stark shift, allowing an efficient mechanical and optical transduction. For typical molecules used in single molecule spectroscopy experiments, this gives an expected electric coupling constant $\alpha \approx 10^{19}$ Hz/m, 4 orders of magnitude larger than the magnetic coupling constant observed in Ref. [8].

In order to show the capabilities of this detection technique, we provide explicit predictions for the luminescence excitation spectrum and the second order photon correlation

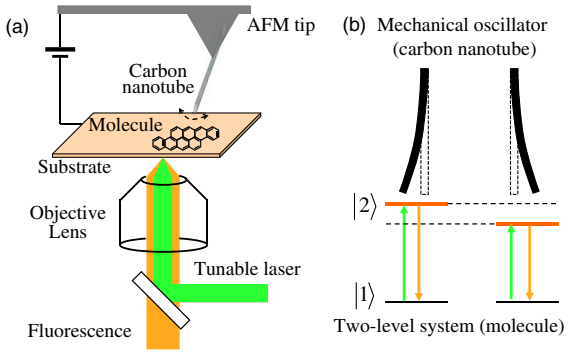

FIG. 1 (color online). Schematic representation of the proposed experiment. (a) Standard far-field confocal microscopy setup for single molecule detection with a carbon nanotube suspended from an AFM tip. (b) Modulation of molecular level splitting during the nanotube oscillations.

function [$g^{(2)}(t)$] of the molecule coupled to the oscillator. We specifically show (i) the modification of the molecular fluorescent excitation spectrum, (ii) the possibility of real time displacement detection, (iii) the relation between $g^{(2)}(t)$ and the oscillator spectrum, which allows using the detection scheme in the nonadiabatic regime, and (iv) the possibility of the backaction cooling of the oscillator.

Model.—Our description of the proposed experiment is based on the Hamiltonian $H = H_M + H_L + H_{\rm phot} + H_{\rm osc} + H_\xi$. Here, $H_M = \hbar\omega(x)\hat{n}$ describes the electronic state of the molecule, modeled as a TLS $\{|1\rangle, |2\rangle\}$, with $\hat{\pi} = |1\rangle\langle 2|$ and $\hat{n} = |2\rangle\langle 2|$. The TLS energy splitting is $\omega(x) = \omega_0 + \Delta\vec{\mu}\cdot\vec{E}(x)/\hbar \approx \omega_0 + \Delta\vec{\mu}\cdot\vec{E}(0)/\hbar + \alpha x$, where ω_0 is the bare level splitting of the molecule, $\Delta\vec{\mu} = \langle 2|\vec{\mu}|2\rangle - \langle 1|\vec{\mu}|1\rangle$ is its permanent electric dipole moment, $\alpha = \partial_x[\Delta\vec{\mu}\cdot\vec{E}(x)]|_{x=0}/\hbar$, and $\vec{E}(x)$ is the electric field at the molecule that depends on the displacement x of the nanotube tip from its equilibrium position. For simplicity, we will focus on a single oscillator mode; thus, x is a scalar. The term $H_L = \Omega_L\hat{\pi}e^{i\omega_L t} + \text{H.c.}$ describes the coupling of the TLS to a laser field of frequency ω_L and with amplitude parametrized by the Rabi frequency Ω_L. The coupling with the photon vacuum environment is given by $H_{\rm phot}$ and leads to a decay rate Γ of the TLS. Finally, $H_{\rm osc} = p_x^2/(2m) + m\omega_M^2 x^2/2$ and H_ξ describe the selected mode of the mechanical oscillator (with resonant frequency ω_M and effective mass m) and its coupling to the thermal environment of temperature T inducing a damping rate γ and stochastic force fluctuations.

Under the usual assumptions of a short memory photon vacuum [17], the equations of motion for the reduced density matrix elements $\sigma_{12} = \sigma_{21}^* = \langle\hat{\pi}\rangle$ and $\sigma_{22} = 1 - \sigma_{11} = \langle\hat{n}\rangle$ of the TLS take the form of Bloch equations:

$$\frac{d\sigma_{12}(t)}{dt} = -i[\delta + \alpha x(t)]\sigma_{12}(t) - \frac{\Gamma}{2}\sigma_{12}(t) + i\Omega_L[2\sigma_{22}(t) - 1], \tag{1a}$$

$$\frac{d\sigma_{22}(t)}{dt} = -2\Omega_L\Im[\sigma_{12}(t)] - \Gamma\sigma_{22}(t), \tag{1b}$$

where $\delta = \omega(0) - \omega_L$ is the detuning.

On the same grounds, the dynamics of the average of x after tracing out the environment degrees of freedom is described by the Langevin equation

$$\frac{d^2x(t)}{dt^2} + \gamma\frac{dx(t)}{dt} + \omega_M^2 x(t) = \frac{\xi(t)}{m} + f_{\rm ba}(t). \tag{2}$$

Here, the force $\xi(t)$ is a Gaussian fluctuating field with $\langle\xi(t)\rangle = 0$ and $\langle\xi(t)\xi(t')\rangle = 2m\gamma k_B T\delta_D(t - t')$ [k_B is the Boltzmann constant and $\delta_D(t)$ is the Dirac delta function]. We restrict to a classical description of the oscillator ($k_B T \gg \hbar\omega_M$) that is the more relevant case for the typical experimental conditions. The last term in Eq. (2) describes the backaction force acting on the oscillator: $mf_{\rm ba}(t) = \hbar\alpha\sigma_{22}(t)$.

We begin by assuming that the backaction force is negligible. The validity of this assumption will be discussed later.

Luminescence excitation spectrum.—The resonant fluorescent excitation spectrum is proportional to the population of the TLS excited state σ_{22}. Solving Eqs. (1) to order Ω_L^2 for $\Omega_L/\Gamma \ll 1$, we obtain

$$\sigma_{22}(t) = \Omega_L^2\left|\int_{-\infty}^{t} dt_1 e^{-i[\delta - i\Gamma/2](t-t_1) - i\alpha\int_{t_1}^{t} d\tau x(\tau)}\right|^2. \tag{3}$$

Equation (3) has to be averaged ($\langle\ldots\rangle_x$) over the displacement fluctuations described by Eq. (2) to obtain the stationary population [16]. For small oscillator damping $\gamma \ll \omega_M, \Gamma$, this gives

$$\langle\sigma_{22}\rangle_x = \Omega_L^2\frac{\Gamma + \Gamma_\phi}{\Gamma}\sum_{n=-\infty}^{+\infty}\frac{e^{-\zeta^2}I_n(\zeta^2)}{(\delta + n\omega_M)^2 + \frac{1}{4}(\Gamma + \Gamma_\phi)^2}, \tag{4}$$

where $I_k(z)$ are the modified Bessel functions, $\zeta^2 = \alpha^2\langle x^2\rangle_x/\omega_M^2$ is an effective TLS oscillator dimensionless coupling constant involving the temperature ($\langle x^2\rangle_x = k_B T/m\omega_M^2$), and $\Gamma_\phi = 2\gamma\zeta^2$ is the TLS mechanically induced dephasing rate.

Figure 2 shows a typical luminescence excitation spectrum obtained from Eq. (4). If not otherwise stated, in the figures and estimates below, we choose the following values of the parameters: $\Gamma/(2\pi) = 10$ MHz, $\Omega_L = 0.1\Gamma$, $m = 10^{-21}$ kg, and the mechanical oscillator quality factor $Q = \omega_M/\gamma = 10^3$. The main feature of the spectrum is the appearance of the sideband peaks at frequencies $\delta \pm n\omega_M$, with n an integer. Their intensity is controlled by ζ through the Bessel functions. For $\zeta \ll 1$, a measure of the oscillator fluctuation can be obtained directly from the ratio of the heights of two subsequent peaks $I_{n+1}(\zeta^2)/I_n(\zeta^2) = \zeta^2/2(n+1)$. It is noteworthy that, for low quality factors (cf. $Q = 10$, which is shown in Fig. 2), the peaks significantly broaden due to the mechanically induced dephasing [16].

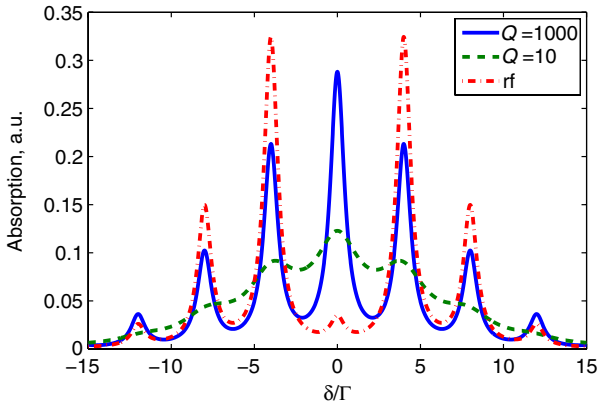

FIG. 2 (color online). Luminescence spectra for the TLS interacting with the oscillator for $\zeta = 1.5$ and $\omega_M = 4\Gamma$.

It is instructive to compare this result to the case of a molecule driven by a perfectly periodic electric signal, such as a radio frequency (rf) field [11,18]. Replacing $\alpha x(t)$ with $\zeta_{\rm rf}\omega_M\cos(\omega_M t)$ in Eq. (3), where $\zeta_{\rm rf}$ is the dimensionless strength of the rf field, one obtains

$$\overline{\sigma_{22}} = \Omega_L^2 \sum_{n=-\infty}^{+\infty} \frac{J_n^2(\zeta_{\rm rf})}{(\delta + n\omega_M)^2 + \frac{1}{4}\Gamma^2}. \tag{5}$$

The overline indicates averaging over the phase of the rf field. For $\zeta_{\rm rf} \ll 1$, the spectra due to Eqs. (5) and (4) essentially coincide for $\zeta_{\rm rf} = \zeta\sqrt{2}$. However, for $\zeta_{\rm rf} \gg 1$, as a function of n, $J_n^2(\zeta_{\rm rf})$ oscillates, which results in the maximum of intensity shifting to the satellite peaks, whereas $I_n(\zeta_{\rm rf}^2/2)$ monotonically decreases. A simple interpretation of this fact can be obtained by averaging Eq. (5) over a Gaussian distribution of $\zeta_{\rm rf}$ [16]. One finds that the result is very similar to Eq. (4), apart from the broadening of the peaks. The spectrum (4) could thus be viewed with good accuracy as the ensemble average of many rf sources with random phases and a Gaussian distribution of the squared amplitude.

Real time position measurement.—In the adiabatic limit $\omega_M \ll \Gamma$, the sideband peaks merge into a single peak, whose maximum shifts proportionally to the oscillator displacement. Treating $\alpha x(t)$ as a time-independent shift in the Bloch equations, one obtains

$$\sigma_{22}(t) = \frac{\Omega_L^2}{[\delta + \alpha x(t)]^2 + \frac{\Gamma^2}{4} + 2\Omega_L^2}. \tag{6}$$

It is thus possible to monitor the real time position of the oscillator by measuring the variation of the luminescence intensity for a given value of the laser frequency: $I[x(t)] = \eta\Gamma\sigma_{22}(t)$, where η is the quantum efficiency of the detector. The change in the intensity in response to the oscillator displacement is

$$G = \frac{\partial I[x(t)]}{\partial x(t)}\bigg|_{x(t)=0} = -\frac{2\eta\Gamma\Omega_L^2\delta\alpha}{(\delta^2 + \frac{\Gamma^2}{4} + 2\Omega_L^2)^2}. \tag{7}$$

An important characteristic of a displacement detector is its "sensitivity"; i.e., the output noise referred back to the input parameter [1]: $\bar{S}_{xx} = \sqrt{S_{II}(0)/G^2}$, where $S_{II}(0)$ is the spectrum of the intensity fluctuations at zero frequency. In the adiabatic regime, one can treat these fluctuations as a Poissonian process of emitting single photons, for which $S_{II}(0) = I[x = 0]$. We thus obtain

$$\bar{S}_{xx} = \frac{1}{2\alpha\sqrt{\eta\Gamma}} \frac{(\delta^2 + \frac{\Gamma^2}{4} + \Omega_L^2)^{3/2}}{\Omega_L|\delta|}. \tag{8}$$

This expression takes its minimum value at $|\delta| = \Omega_L\sqrt{2} = \Gamma/2$. Taking $\alpha = 10^{19}$ Hz/m and $\eta = 0.01$, we obtain $\bar{S}_{xx} = \sqrt{27/8}\sqrt{\Gamma/\eta}/\alpha \sim 10$ fm/$\sqrt{\rm Hz}$. This is on par with the best values of sensitivity obtained by noninterferometric displacement detection methods [19]. With respect to the latter, the important advantage of the proposed setup is its "open" nature, which allows a simpler integration of the mechanical resonator with other systems.

Another essential characteristic of a detector is its resolution $\Delta x = \bar{S}_{xx}/\sqrt{\Delta t}$, i.e., the smallest displacement that can be measured [1]. Here, Δt is the measurement time, which, in the case of a damped harmonic oscillator, Eq. (2), can be as long as $\gamma^{-1} = Q/\omega_M$. Thus, for the typical nanotube oscillator frequencies in the range of 1 kHz–10 MHz and quality factor $Q = 10^3$, the resolution will vary from 10 fm to 1 pm, which again matches the values obtained by state of the art noninterferometric detection devices [19]. The device can be also used to perform real time displacement detection, without assuming a slowly damped oscillatory behavior of $x(t)$. In order to have a sufficient signal to noise ratio, in this case, the limitation on the oscillator frequency is even more severe, giving $\omega_M \ll [\Gamma/(\alpha\bar{S}_{xx})]^2 = 1$ MHz, where we also used the condition of validity of the linear expansion $\alpha x \ll \Gamma$.

Second order photon correlation function.—In the most common situations, where one is interested in statistical characteristics rather than the exact time evolution of the oscillator, one can resort to the measurement of the second order photon correlation function $[g^{(2)}(t, t')]$ [17] that is obtained by averaging over many two-photon events. We will show that this allows us to improve the frequency resolution even beyond Γ. The measured signal for $g^{(2)}(t, t')$ reads

$$g^{(2)}(t, t') = \frac{\langle\langle \hat{\pi}^\dagger(t')\hat{\pi}^\dagger(t)\hat{\pi}(t)\hat{\pi}(t')\rangle\rangle_x}{\langle\sigma_{22}(t')\rangle_x\langle\sigma_{22}(t)\rangle_x}. \tag{9}$$

At equal times, $g^{(2)}(t, t)$ vanishes ($\hat{\pi}^2 = 0$) since two photons cannot be emitted by a single molecule simultaneously (antibunching). For large times ($\tau = t - t' \gg \Gamma^{-1}$), the photon emission events are no more quantum correlated and the degree of second order coherence reduces to the classical correlation function for the excited state occupation number: $g^{(2)}(t, t') \approx \langle\sigma_{22}(t)\sigma_{22}(t')\rangle_x/\langle\sigma_{22}\rangle_x^2$. For vanishing coupling to the oscillator and at lowest order in Ω_L, $g^{(2)}(t, t')$ exhibits decaying oscillations at the detuning frequency δ:

$$g^{(2)}(\tau) = 1 + e^{-\Gamma\tau} - 2\cos(\delta\tau)e^{-\Gamma\tau/2}. \tag{10}$$

It is possible to obtain analytical expressions for $g^{(2)}(t, t')$ in the presence of the oscillator at lowest order in $\Omega_L/\Gamma \ll 1$ and $\zeta \ll 1$ [16]. The result is in general complex, but in some regimes it has a simple and interesting interpretation. For $\delta = \omega_M$, we find that the free oscillations described by Eq. (10) are in counterphase with those induced by the oscillator, leading to a reduction of the amplitude of the oscillations for $\tau\Gamma \sim 1$ (cf. Fig. 3). For $\Gamma\tau \gg 1$, the Rabi oscillations of Eq. (10) die out and the remaining time dependence is all due to the time correlations induced by the oscillator $\langle\sigma_{22}(t)\sigma_{22}(t')\rangle_x$.

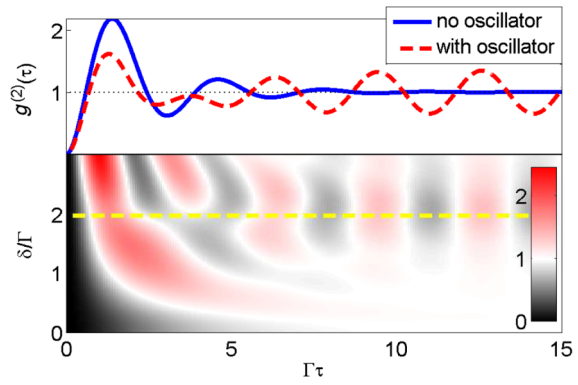

FIG. 3 (color online). Top: $g^{(2)}(\tau)$ as a function of time for $\delta = \omega_M = 2\Gamma$ without and with coupling to the oscillator. Bottom: Color plot of $g^{(2)}(\tau)$ as a function of time and detuning. The dashed line marks $\delta = \omega_M$. The parameters include $\omega_M = 2\Gamma$, $\zeta = 0.15$, and $Q = 10^3$.

This is particularly interesting in the case of fast oscillators $\omega_M \gg \Gamma \gg \gamma$ for which we find

$$g^{(2)}(\tau) = 1 + \frac{4\zeta^2\omega_M^2}{\Gamma^2} e^{-\gamma\tau/2} \cos(\omega_M\tau - Q^{-1}). \quad (11)$$

The amplitude of $g^{(2)}$ thus gives a direct measure of the average amplitude fluctuation of the oscillator. In the opposite limit $\omega_M \ll \Gamma$, one obtains

$$g^{(2)}(t, t') = 1 + \left(\frac{G}{I}\right)^2 \langle x(t)x(t')\rangle_x, \quad (12)$$

valid for an arbitrary oscillator correlation function.

Current-induced dissipation.—The strong coupling between the NT and the TLS is possible due to the large electric field between the NT tip and the conducting substrate [16]. Oscillations thus induce dissipative electric currents. One can single out two different contributions from the currents flowing in the nanotube and in the substrate. We find that the dominant effect comes from the surface losses and that for typical parameters the increase in the oscillator damping rate is $1/(z^3\sigma_{\rm sub})$ GHz nm^3 S/m, where $\sigma_{\rm sub}$ is the substrate conductivity and z is the distance from the substrate. Thus, even if it is possible to minimize this contribution by using highly conducting substrates, in a common situation it is likely that the quality factor of the oscillator will be reduced.

Backaction and the effective temperature.—Let us now discuss in more detail the role of the backaction force. Its effect is controlled by two parameters, the intensity of the force (measured by the ratio between the displacement induced in the equilibrium position of the oscillator $\hbar\alpha/m\omega_M^2$ and $\sqrt{\langle x^2\rangle_x}$) and the frequency and duration of its fluctuation. In order to estimate its average effect, taking both parameters into account, we resort to the linear backaction theory [20]. Within this approach, the action of the TLS on the oscillator can be obtained by evaluating the fluctuation spectrum of the force ($\hbar\alpha\hat{n}$) in the absence of the mechanical oscillator. This is proportional to

$$S_{nn}(\omega) = \int dt e^{i\omega t}\langle\tilde{n}(t)\tilde{n}(0)\rangle = \frac{\Gamma\langle\hat{n}\rangle}{(\delta-\omega)^2 + \frac{\Gamma^2}{4}}, \quad (13)$$

where $\langle\hat{n}\rangle = \Omega_L^2/(\delta^2 + \Gamma^2/4)$ and $\tilde{n} = \hat{n} - \langle\hat{n}\rangle$. For $Q \gg 1$, one can show [20] that the oscillator fluctuations can then be fully characterized by an effective temperature ($T_{\rm osc}$) defined by

$$\coth\left(\frac{\hbar\omega_M}{2k_BT_{\rm osc}}\right) = \frac{\gamma\coth(\frac{\hbar\omega_M}{2k_BT}) + \gamma_1\coth(\frac{\hbar\omega_M}{2k_BT_{\rm TLS}})}{\gamma+\gamma_1}, \quad (14)$$

where $T_{\rm TLS} = \hbar\omega_M S_{nn}^+/[2k_BS_{nn}^-]$, $\gamma_1 = (\alpha x_{zpf})^2 S_{nn}^-$, $S_{nn}^{\pm} = S_{nn}(\omega_M) \pm S_{nn}(-\omega_M)$, and $x_{zpf} = \sqrt{\hbar/(2m\omega_M)}$. When $\gamma_1 \gg \gamma$, the oscillator temperature is completely determined by $T_{\rm TLS}$, which in turn is controlled by the detuning δ. For positive values of δ, i.e., for the photon energies below the transition energy, this results in cooling the oscillator down to the temperature $T_{\rm TLS}$ [21,22]. At the optimal value $\delta = \sqrt{\omega_M^2 + \Gamma^2/4}$, we obtain $T_{\rm TLS} = \hbar\Gamma/(4k_B)$ for $\omega_M \ll \Gamma$ and $T_{\rm TLS} \approx \hbar\omega_M/[2k_B\log(4\omega_M/\Gamma)]$ in the resolved sideband limit $\omega_M \gg \Gamma$. Note that, unlike in the case of coupling to a photon cavity [21,22], where one can infinitely increase the number of cavity photons, the population of the excited state ($\langle\hat{n}\rangle$) entering linearly the expression for γ_1 saturates at high laser strengths and remains smaller than one-half.

The effective temperature expression (14) holds for $\gamma_1 \ll \Gamma$ [21], whereas cooling requires that $\gamma_1 \gg \gamma$. In the resolved sideband limit, these conditions result in [16] $\sqrt{\gamma\Gamma/\langle n\rangle} \ll \alpha x_{zpf} \ll \Gamma/\sqrt{\langle n\rangle}$, whereas for $\omega_M \ll \Gamma$ the conditions read the same, but with x_{zpf} replaced by $\sqrt{\hbar/(2m\Gamma)}$. For $\omega_M \approx \Gamma$, we thus obtain that the linear response description is correct for $\alpha < 10^{19}$ Hz/m, i.e., under all realistic circumstances, whereas the backaction

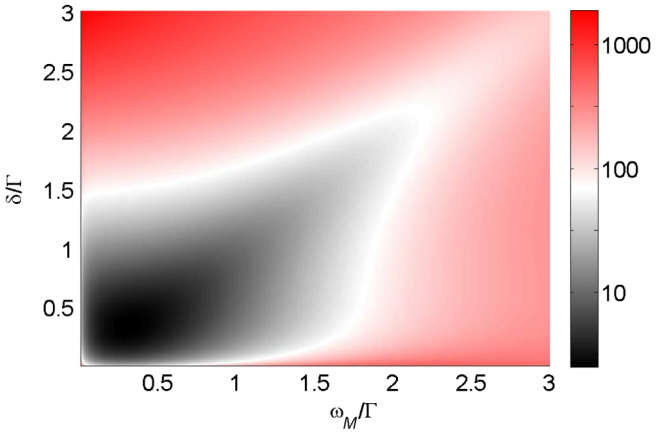

FIG. 4 (color online). The ratio $k_BT_{\rm osc}/(\hbar\omega_M)$ as the function of the detuning and the oscillator frequency for $\alpha = 10^{19}$ Hz/m and $T = 1$ K ≈ 22 GHz.

effects are negligible for $\alpha \ll 10^{17}$ Hz/m. This gives the quantitative condition for discarding f_{ba} in the first part of this Letter. This also indicates that there is a window of at least 2 orders of magnitude of the coupling constant where the backaction can be used to conveniently manipulate the oscillator. The dependence of the effective temperature on δ/Γ and ω_M/Γ is shown in Fig. 4: The temperature of the oscillator can be reduced by a factor of 1000 when $\omega_M/\Gamma \approx 0.1$–$0.4$.

Conclusion.—In this Letter, we have shown that single molecule spectroscopy can be used as an efficient tool for detecting and manipulating nano-oscillators, such as carbon nanotubes attached to an AFM tip and interacting with the molecule via electrostatic forces. We analyzed different detection schemes, which allow for obtaining either real time or averaged information on the oscillator displacement, and estimated very large values of the coupling constant, which allow for reaching a high detection efficiency. Furthermore, the backaction of the molecule on the oscillator can be made sufficiently large to enable strong cooling of the oscillator with the proposed setup. We considered in this Letter only the linear part of the TLS oscillator coupling, but by properly positioning the nanotube it is possible to work in a regime where the dominant coupling is quadratic, leading to the wide range of possibilities including that of measuring the energy of the oscillator [23]. Single molecule spectroscopy appears thus as a promising new technique for detecting displacement and exploring strong coupling regimes of a driven two-level system with a nanomechanical oscillator.

F. P. and V. P. acknowledge financial support from the Région Aquitaine through Contract No. 20101101013 and the French ANR through Contract QNM No. 040401. B. L. acknowledges financial support from the ANR and the ERC.

[1] M. Poot and S. H. J. van der Zant, Phys. Rep. **511**, 273 (2012).

[2] M. P. Blencowe and M. N. Wybourne, Appl. Phys. Lett. **77**, 3845 (2000); R. G. Knobel and A. N. Cleland, Nature (London) **424**, 291 (2003); M. D. LaHaye, O. Buu, B. Camarota and K. C. Schwab, Science **304**, 74 (2004); A. Naik, O. Buu, M. D. LaHaye, A. D. Armour, A. A. Clerk, M. P. Blencowe, and K. C. Schwab, Nature (London) **443**, 193 (2006).

[3] S. Etaki, M. Poot, I. Mahboob, K. Onomitsu, H. Yamaguchi, and H. S. J. van der Zant, Nat. Phys. **4**, 785 (2008); O. Usenko, A. Vinante, G. Wijts, and T. H. Oosterkamp, Appl. Phys. Lett. **98**, 133105 (2011); M. D. Lehaye, J. Suh, P. M. Echternach, K. C. Schwab, and M. L. Roukes, Nature (London) **459**, 960 (2009).

[4] A. D. O'Connell *et al.*, Nature (London) **464**, 697 (2010).

[5] N. E. Flowers-Jacobs, D. R. Schmidt, and K. W. Lehnert, Phys. Rev. Lett. **98**, 096804 (2007); M. R. Kan, D. C. Fortin, E. Finley, K.-M. Cheng, M. R. Freeman, and W. K. Hiebert, Appl. Phys. Lett. **97**, 253108 (2010).

[6] O. Arcizet, P.-F. Cohadon, T. Briant, M. Pinard, and A. Heidmann, Nature (London) **444**, 71 (2006); O. Arcizet, P.-F. Cohadon, T. Briant, M. Pinard, A. Heidmann, J.-M. Mackowski, C. Michel, L. Pinard, O. Français, and L. Rousseau, Phys. Rev. Lett. **97**, 133601 (2006); M. Poggio, C. L. Degen, H. J. Mamin, and D. Rugar, Phys. Rev. Lett. **99**, 017201 (2007); A. Vinante *et al.*, Phys. Rev. Lett. **101**, 033601 (2008); S. Groblacher, J. B. Hertzberg, M. R. Vanner, G. D. Cole, S. Gigan, K. C. Schwab, and M. Aspelmeyer, Nat. Phys. **5**, 485 (2009); S. Stapfner *et al.*, arXiv:1211.1608v1.

[7] J. D. Teufel, T. Donner, D. Li, J. W. Harlow, M. S. Allman, K. Cicak, A. J. Sirois, J. D. Whittaker, K. W. Lehnert, and R. W. Simmonds, Nature (London) **475**, 359 (2011).

[8] O. Arcizet, V. Jacques, A. Siria, P. Poncharal, P. Vincent, and S. Seidelin, Nat. Phys. **7**, 879 (2011).

[9] P. Rabl, P. Cappellaro, M. Dutt, L. Jiang, J. Maze, and M. Lukin, Phys. Rev. B **79**, 041302(R) (2009); P. Rabl, Phys. Rev. B **82**, 165320 (2010); Sh. Kolkowitz, A. C. Bleszynski Jayich, Q. P. Unterreithmeier, S. D. Bennett, P. Rabl, J. G. E. Harris, and M. D. Lukin, Science **335**, 1603 (2012).

[10] T. Basché, W. E. Moerner, M. Orrit, and U. P. Wild, *Single Molecule Optical Detection, Imaging and Spectroscopy* (VCH, Weinheim, 1997).

[11] Ph. Tamarat, A. Maali, B. Lounis, and M. Orrit, J. Phys. Chem. A **104**, 1 (2000).

[12] Ch. Brunel, Ph. Tamarat, B. Lounis, J. C. Woehl, and M. Orrit, J. Phys. Chem. A **103**, 2429 (1999).

[13] W. E. Moerner, T. Plakhotnik, T. Irngartinger, U. Wild, D. Pohl, and B. Hecht, Phys. Rev. Lett. **73**, 2764 (1994).

[14] M. Fauré, B. Lounis, and A. Buzdin, Europhys. Lett. **77**, 17 005 (2007).

[15] R. C. Smith, D. C. Cox, and S. R. P. Silva, Appl. Phys. Lett. **87**, 103112 (2005).

[16] See Supplemental Material at http://link.aps.org/supplemental/10.1103/PhysRevLett.110.125501 for the details of the derivation.

[17] R. Loudon, *The Quantum Theory of Light* (Oxford University Press, New York, 2000), 3rd ed.

[18] Ch. Brunel, B. Lounis, Ph. Tamarat, and M. Orrit, Phys. Rev. Lett. **81**, 2679 (1998).

[19] See Table 7 in Ref. [1].

[20] A. A. Clerk, Phys. Rev. B **70**, 245306 (2004); A. A. Clerk and S. Bennett, New J. Phys. **7**, 238 (2005).

[21] F. Marquardt, J. P. Chen, A. A. Clerk, and S. M. Girvin, Phys. Rev. Lett. **99**, 093902 (2007).

[22] M. I. Dykman, Sov. Phys. Solid State **20**, 1306 (1978); V. B. Braginsky and S. P. Vyatchanin, Phys. Lett. A **293**, 228 (2002); F. Marquardt, J. P. Chen, A. A. Clerk, and S. M. Girvin, Phys. Rev. Lett. **99**, 093902 (2007); I. Wilson-Rae, N. Nooshi, W. Zwerger, and T. J. Kippenberg, Phys. Rev. Lett. **99**, 093901 (2007); C. Genes, D. Vitali, P. Tombesi, S. Gigan, and M. Aspelmeyer, Phys. Rev. A **77**, 033804 (2008).

[23] V. B. Braginsky, Y. I. Vorontsov, and K. S. Thorne, Science **209**, 547 (1980); J. D. Thompson, B. M. Zwickl, A. M. Jayich, F. Marquardt, S. M. Girvin, and J. G. E. Harris, Nature (London) **452**, 72 (2008).